Fixing the Boundaries for Causal Dynamical Triangulations in 2+1 Dimensions

Jonah M. Miller *
Department of Physics
University of Colorado
Boulder, CO 80309

October 2, 2012

Abstract

In this paper, we modify the discrete Regge action of Causal Dynamical Triangulations (CDT) to account for fixed boundary conditions on the spacetime manifold and to include an appropriate boundary term. We demonstrate that the resulting geometries agree with previous results from CDT with periodic boundary conditions—and more importantly, reduce to classical general relativity in the appropriate limit. We further propose a number of interesting questions that fixed-boundaries CDT may be able to answer.

1 Introduction

1.1 The Problem of Quantum Gravity

An important question in modern physics is this:

> How do we merge the theories of quantum mechanics and general relativity to produce a physically meaningful theory of quantum gravity?

For a theory to be physically meaningful, it must agree with previous experimental results and offer new, testable predictions. Currently, every theory of quantum gravity falls short of meeting both these criteria [1].

A major challenge of merging the two theories is reconciling the fundamental assumptions that each theory makes. Quantum mechanics assumes that fields (or particles, if you like) evolve in time on a fixed background. Einstein's theory of gravity, on the other hand, treats the background itself as a dynamical object. Space and time bend, curve, and reshape themselves according to the

*jonah.maxwell.miller@gmail.com

mass and energy contained in the universe. Since the fields themselves are affected by changes in background geometry, treating fields on a dynamical background has proven to be a major challenge [1].

Several competing theories that attempt to build a coherent picture of quantum gravity have emerged, including string theory and loop quantum gravity. However, as of yet, these theories fail to meet all the criteria required for a physically meaningful theory. One could continue to work on solving quantum gravity analytically, perhaps by continuing to study string theory or a similar approach, or one could argue that these theories have more demanded of them than is fair [1, 2].

It is possible that the problem of quantum gravity is currently too hard and an analytic solution must wait. Rather than attempt to solve all of quantum gravity at once, it might be more feasible to attempt to gain insight from simpler models or numeric results [3, 1, 4].

Causal Dynamical Triangulations (CDT) is a method through which we hope to gain some insight into the problem of quantum gravity. It is a method that finds the expected quantum universe by translating the Feynman path integral into an integral over all possible space-times. CDT has already reproduced the correct functional form for the vacuum solution of Einstein's equations [3, 5, 6, 7, 8] and appears to be a promising approach to quantizing gravity [9, 2, 10].

Although it is technically possible to approach CDT analytically, this appears intractable for dimensions higher than 1+1. Instead, we approach the problem numerically. This results in a statistical numerical model of quantum gravity [3].

This paper deals with CDT in 2+1 dimensions, as opposed to the 3+1 dimensions of Einstein's theory of gravity or the higher dimensions of string theory. We reduce the number of dimensions for the same reason that we attempt a numerical rather than analytical model: It is easier to extract physical insight from a simpler model. So far, the results are promising.

1.2 Overview

In this paper, I will briefly discuss the theory required for understanding Causal Dynamical Triangulations in 2+1 dimensions, why it is useful, and what I accomplished over the summer. I will discuss background information: the discretization of gravity, the discretization of spacetime, how to change spacetime, and the algorithm for generating an ensemble of quantum spacetimes. Then I will discuss my own research: the analytic derivation of the discretized Regge action with fixed boundaries and the results of fixed-boundaries Monte Carlo simulations.

2 Quantizing Gravity by Path Integral

CDT's approach to quantum gravity is to adapt Feynman's path-integral formalism to gravity. Classically, as shown in figure 1, a particle takes a single path between two points.[1] However, a quantum particle is a wave and thus de-localized. In some sense, it takes every possible path between two points; the shortest path is simply the most likely path [11]. To account for this,

[1] It is important to note that these points are, in general, functions of time.

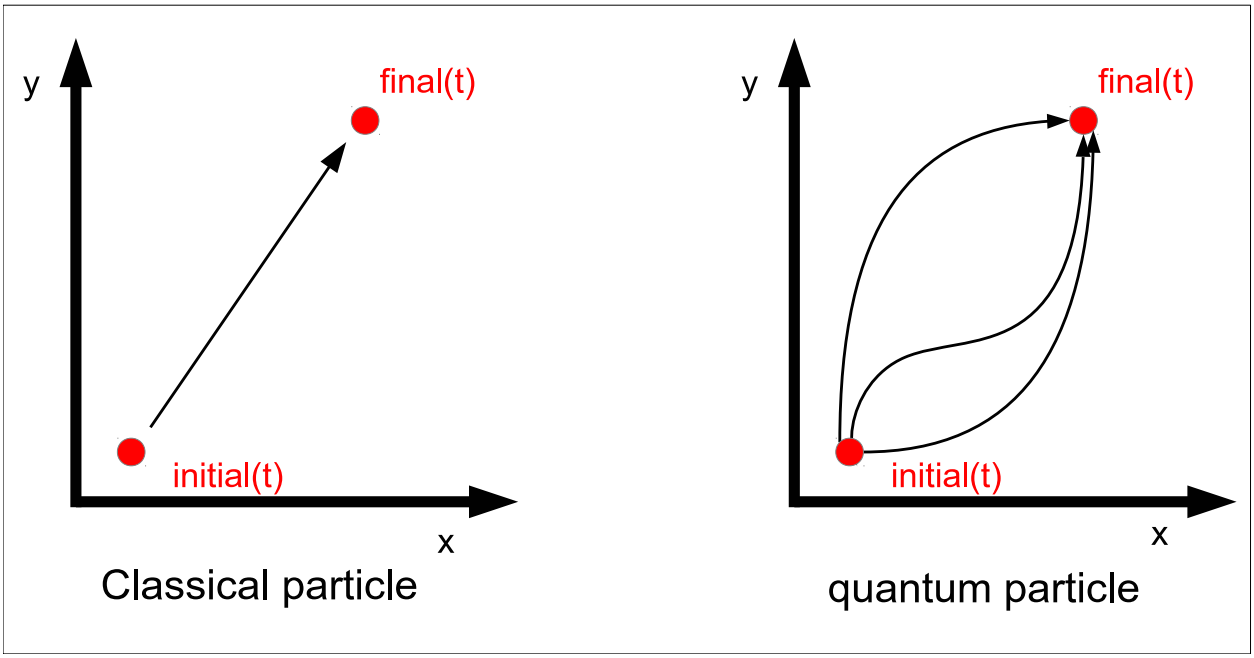

Figure 1: A classical particle (left) takes a single path between two points (each a function of time), while a quantum particle (right) takes every possible path.

we must sum over all possible paths from an initial point to a final point in order to calculate the probability of a particle traveling between those points [11].

Formally, a path integral is usually written as

$$Z = \int_{x_0}^{x_1} [\mathscr{D}x] e^{iS[x]/\hbar}, \tag{1}$$

where

$$S[x] = \int_{t_0}^{t_1} dt L[x(t)] \tag{2}$$

is the action of the system, and $L = KE - PE$ is the Lagrangian [11]. $[\mathscr{D}x]$ does not mean the differential form of the coordinates x, but the differential form of all possible paths between endpoints x_0 and x_1. The idea is to sum over every path, weighting the value of each path by its amplitude.[2] The term with the action in it, $e^{iS/\hbar}$, is meant to weight each path [11]. With some logical leaps, we can extend this idea to gravity.

In gravity, the initial and final "points" x_0 and x_1 are the initial and final geometries of the spatial dimensions of the universe [1]. Each "path" is a possible shape that space-time could form to connect the initial and final geometries [1]. Each of these shapes is called a *history*, since it

[2] I mean amplitude in the quantum mechanics matter wave sense. Intuitively, though not rigorously, the amplitude of path p is the likelihood a particle will take p.

represents one possible history of the universe [1]. In natural units,[3] the path integral thus becomes

$$Z = \int_{\mathscr{G}} [\mathscr{D} g_{\mu\nu}] e^{iS[g_{\mu\nu}]}, \tag{3}$$

where $g_{\mu\nu}$ is the metric tensor and $\mathscr{G}$ represents the space of all possible geometries of the Lorentzian spacetime[3]. Instead of the action for a classical particle, we use the Einstein-Hilbert action

$$S^{EH} = \frac{1}{16\pi G} \int_{\mathscr{M}} (R - 2\Lambda) \sqrt{-g} d^D x, \tag{4}$$

where G is Newton's constant, $\mathscr{M}$ is the spacetime manifold in question, R is the Ricci scalar, g is the determinant of the metric tensor, Λ is the cosmological constant, and D is the number of dimensions of gravity the theory works with [3, 12, 13, 14]. D is usually 4, but we will work with $D = 3$.

If the spacetime is to have boundaries (such as initial and final geometries), then we must add the Gibbons-Hawking-York boundary term to the action:

$$S^{GHY} = \frac{1}{8\pi G} \int_{\partial \mathscr{M}} d^{D-1} x \sqrt{\gamma} K, \tag{5}$$

where $\partial \mathscr{M}$ is the boundary submanifold of the spacetime, γ is the determinant of the induced metric on the boundary, and K is the trace of the extrinsic curvature tensor [13].[4] Thus, for non-closed manifolds, the full action used in the path integral is [13]:

$$\begin{aligned} S_{continuous} &= S^{EH} + S^{GHY} \\ &= \frac{1}{16\pi G} \int_{\mathscr{M}} (R - 2\Lambda) \sqrt{-g} d^D x + \frac{1}{8\pi G} \int_{\partial \mathscr{M}} d^{D-1} x \sqrt{\gamma} K. \end{aligned} \tag{6}$$

It is worth noting that in previous work on CDT, the initial and final geometries were identified and the system was given periodic boundary conditions. In the periodic case, the Gibbons-Hawking-York term is zero and equation (4) completely describes the system. However, in the present work, we do not use periodic boundary conditions, and the boundary term will become important.

3 Putting the Universe on Your Desktop

Up to this point, we've glossed over what it means to integrate over all possible spacetimes that connect the initial and final geometries. In our case, we discretize the path integral and perform the sum on a computer. Of course, we can't possibly put every history in this infinite set with its weight into the computer and sum over all of them. However, we can put a large enough number of the likeliest histories into the computer and sum over those. Ideally, the contribution of the omitted histories is small enough that the resulting sum converges in a physically meaningful way [3, 4, 1].

The major challenges of this procedure are discretizing space-time in a way a computer can understand, and discretizing the action.

[3] In natural units, $c = \hbar = 1$. In this paper, unless otherwise stated, we will always use natural units.

[4] Mathematicians call the extrinsic curvature the Second Fundamental Form.

3.1 Regge Calculus: Discretizing Space-Time

In theory, it is possible to approximate a manifold using a discrete number of points and a metric function defined on those points. However, a more efficient method of discretizing space-time is the coordinate-free method proposed by Regge [15, 12].

In coordinates, one calculates curvature at each point by performing parallel transport for a vector V^μ in an infinitesimally small closed loop around that point in a special way. We contain the loop in the plane and define it by two vectors, A^μ and B^ν. We then parallel transport the vector along A^μ and B^ν and complete the loop by transporting along $-B^\nu$ and $-A^\mu$. The change in the vector due to parallel transport is thus

$$\delta V^\rho = R^\rho{}_{\sigma\mu\nu} V^\sigma A^\mu B^\nu, \tag{7}$$

where $R^\rho{}_{\sigma\mu\nu}$ is the Riemann curvature tensor [14].

In Regge's formulation, we use a discrete, more rough-grained method. If we discretize a manifold so that it is piecewise flat (continuous, but constructed of flat submanifolds), then we can define a *bone*. A bone is a (D-2)-dimensional submanifold in which all curvature is concentrated. Around each bone, we measure a *deficit angle*. For a simplicial manifold (a manifold made up of D-dimensional simplices), a bone is a (D-2)-simplex and the deficit angle is failure of the angle around the bone to equal 2π [15, 12].

Formally, the integrated curvature over a region can be approximated with

$$\frac{1}{2}\int_{region} \sqrt{g} R d^D x = \sum_{b \in region} V(b)\delta_b, \tag{8}$$

where *region* is the region bounded by a closed curve, D is the dimension of the space, R is the Ricci scalar, $g = \det(g_{\mu\nu})$ is the determinant of the metric, b indexes bones, V is the D-dimensional analogue of volume for a bone's length if $D = 3$, area if $D = 2$, etc., and δ_b is the deficit angle around a given bone. By definition, V is unity if $D = 2$ [15, 12].

Although Regge proves this relation in his paper, an intuitive explanation might be in order. (A more detailed explanation can be found in the chapter on Regge Calculus in [12] and Regge's original paper in [15].) In two dimensions, we can calculate the *total curvature*[5] of a region bounded by a closed curve by how much a vector parallel transported around the entire loop changes. Indeed, if we construct our loop out of three geodesics to form a perfect triangle as shown in figure 2(A), then the total curvature is uniquely determined by the failure of the interior angles of the triangle to add up to π [16].

For a two-dimensional manifold, in a very rough, intuitive sense, the bone is the area bounded by a closed curve, and the "volume" of this bone is an infinitesimal volume element over which we are integrating. The equivalent to calculating the curvature at a point x on a sphere is shown in figure 2(B) and (C). The curvature at point x is calculated by finding the deficit angle for a closed curve bounding x. In the discrete case, this deficit angle is found by simply summing up the angles of the triangles that contain x as a vertex around x and finding their deviation from 2π.

[5] The Ricci scalar integrated over a region

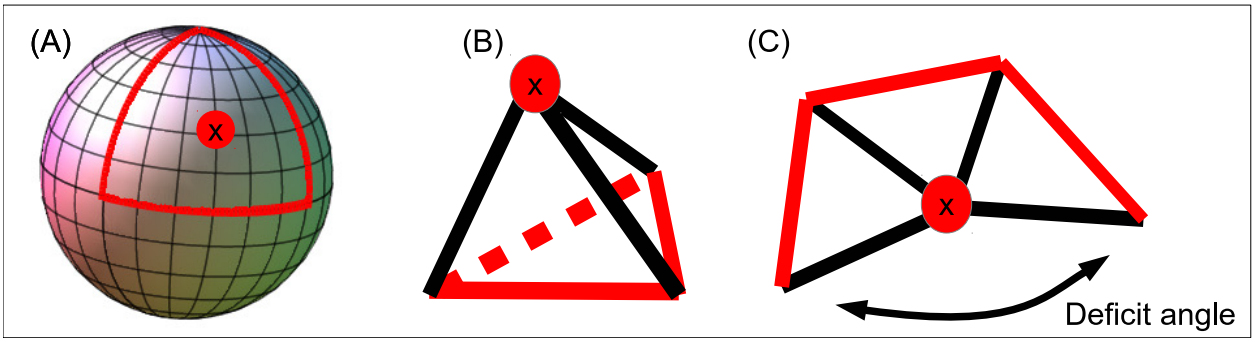

Figure 2: (A) A perfect triangle, shown in red, can be used to measure the curvature in a bounded region on a sphere. (B) A tetrahedron is a very crude approximation of a sphere. (C) Somewhat analogously to the use of a perfect triangle, we can find the curvature at a vertex x on the tetrahedron—which is a bone for two-dimensional simplicial manifolds—by finding the deviation from 2π of the full angle of rotation around the bone. We call this deviation the *deficit angle*.

It is important to note that the deficit angle of Regge's formulation is only path independent because the manifold is piecewise flat. In a piecewise flat manifold, all curvature is concentrated in the bones. Thus, the precise points contained in the area bounded by the path are irrelevant as long as the path goes around the bone. In general, curvature can be distributed throughout the manifold and parallel transport is path-dependent [12, 16].

In CDT, we construct our discretized manifold entirely out of simplices,[6] of a finite number of types. In this case, the question of summing up angles becomes a question of counting simplices that contain a bone[7] [3]. It is important to note that Regge calculus does not demand that a manifold be triangulated by equilateral simplices. Regge envisioned the lengths of individual bones and simplices changing to reflect curvature change [15, 12]. CDT's method of adding and removing simplices is a computational simplification added later. We will describe the simplices we use in 2+1-dimensional CDT in a later section. However, we must first address some global concerns.

3.2 Putting the "Causal" in Causal Dynamical Triangulations

There are three properties of CDT that make it a causal theory. The first and most obvious is that all manifolds are Lorentzian manifolds, with an indefinite metric and one time dimension. One consequence is that angles around space-like bones can be complex. The length-squared of a time-like vector is negative, so the angle between a space-like vector x^μ and a time-like vector y^μ is [3]:

[6] A simplex is a generalized triangle. Points, lines, triangles and tetrahedra are the simplices that can be embedded in 3 dimensions.

[7] A bone is a vertex for $D = 2$, and edge for $D = 3$, a 2-dimensional face for $D = 4$, and so on.

$$\theta = \arccos\left[\frac{x^\mu y_\mu}{\sqrt{x_\nu x^\nu y_\sigma y^\sigma}}\right] = \arccos\left[\frac{-|x^\mu y_\mu|}{i\sqrt{|x_\nu x^\nu y_\sigma y^\sigma|}}\right] \in \mathbb{C}. \tag{9}$$

If we wish to preserve causal structures, it is important to preserve this property [1].

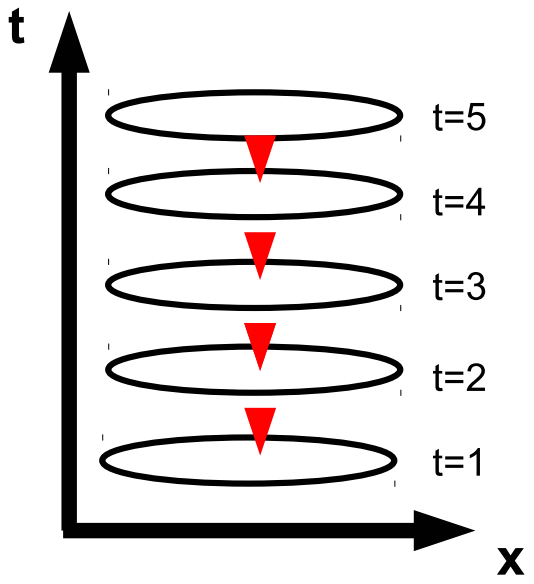

Figure 3: A time foliation of space-time. We enforce a preferred proper time by separating the universe into space-like manifolds at each proper time.

The second and third properties of CDT that make it a causal theory enforce a sort of "global causality." They are niceness conditions that were absent in the previous theory, Dynamical Triangulations, which caused the path integral to behave badly [3, 1, 4]. The first niceness condition is to enforce a time foliation on all space-times and allow only space-times that permit a foliation into the path integral. Intuitively, a time foliation is a partitioning of the universe into space-like manifolds, each at a proper time t, as shown in figure 3 [1].

The second niceness condition is a restriction on topological changes. At each proper time t, the spatial geometry must have the same topology as the spatial geometries at each other time. For example, if the topology of the space at time $t = 0$ is a sphere S^{D-1}, then the topology at $t = 1$ cannot be a torus. This prevents wormholes and baby universes from entering a space-time [1]. Figure 4 shows the types of space-time that the two niceness conditions prevent from entering the path integral.

Formally, these two niceness conditions on a D-dimensional manifold $\mathscr{M}$ mean that for any finite time interval I, we can write the topology of the manifold as

$$\mathscr{M} = I \times \Sigma \tag{10}$$

where Σ is any $(D-1)$-dimensional manifold.

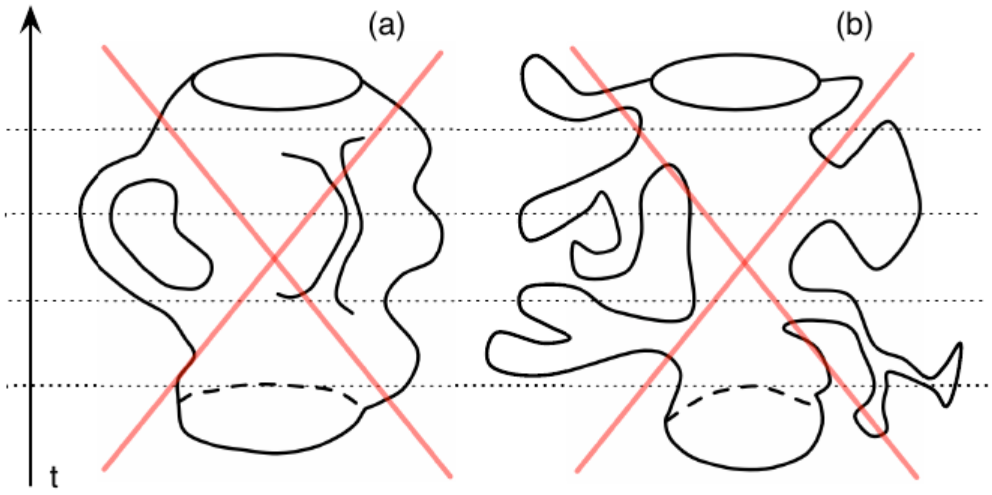

Figure 4: Two types of universes not allowed by CDT: (a) wormholes and (b) baby universes. Image from [1].

3.3 The Building Blocks of CDT in 2+1 Dimensions

We are now ready to discuss how a space-time is actually constructed in 2+1-dimensional CDT. We will first discuss the types of simplices used to build a space-time, then discuss the so-called ergodic moves, which change a space-time.

3.3.1 Types of 3-Simplices

In 2+1-dimensional CDT, space-time is constructed of equilateral tetrahedra. In general, the space-like edges of the tetrahedra are of length-squared a and the time-like edges are of length-squared $-\alpha a$. However, a is just a scale factor and we can take $a = 1$ without loss of generality.[8] In $2+1$ dimensions, α is also arbitrary and we can, without loss of generality, let $\alpha = 1$ as well.[9] Thus, in $2+1$-dimensional CDT, spacetime is made of equilateral tetrahedra.

Although these tetrahedra are identical up to rigid motion, the time-foliation condition introduces three separate orientations which must be treated differently [3, 1].[10] Figure 5 shows the three orientations: the $(3,1)$-, $(2,2)$-, and $(1,3)$-simplices. Each tetrahedron is suspended between two proper times, and the space-like faces of the $(3,1)$- $(1,3)$-simplices triangulate the spatial geometry of the universe at each proper time. The simplices are named for how many vertices are located at what proper time. The $(3,1)$-simplex has three vertices in the lower time slice and one in the upper time slice; the $(2,2)$-simplex has two vertices in each time slice; and the $(1,3)$-

[8] We will let $a = 1$ for the remainder of this paper.

[9] α is not arbitrary $3+1$ dimensions.

[10] There are *three* orientations instead of *two* because foliation introduces not only a preferred time axis, but also a preferred time direction, or *arrow of time.*

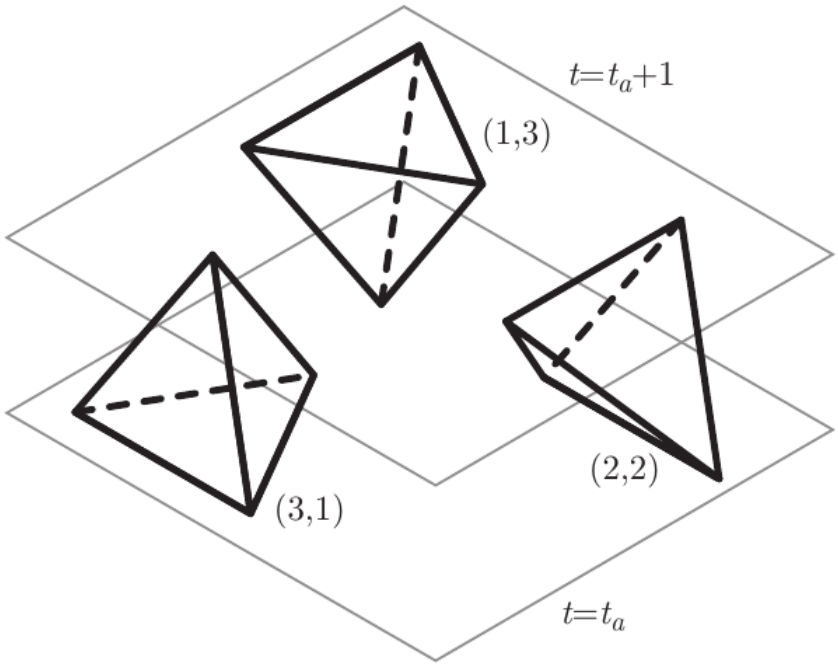

Figure 5: The three types of simplex used in 2+1-dimensional CDT. Each type is referred to by how many vertices it has in a given time slice. The $(3,1)$-simplex has three vertices in the lower time slice and on in the upper time slice. The $(2,2)$-simplex has two vertices in each time slice, and the $(1,3)$-simplex is a $(3,1)$-simplex, but upside-down. All three simplices are identical up rigid motion. Image from [2].

simplex is a $(3,1)$-simplex, but upside-down [3]. For a space-time to be acceptable, all simplectic "building blocks" must meet at triangular faces and all faces must be intersection points. The only exception is at the boundary. Space-like triangles at the boundary may be contained by only one $(3,1)$- or $(1,3)$-simplex [3]. Let the norm-squared of a space-like edge of our tetrahedra be $a = 1$ and let the norm-squared of a time-like edge be $-\alpha a = -\alpha$. Note that in general $\alpha \neq 1$. In the 2+1-dimensional case, the value of α is irrelevant, so we choose it to be 1. However, in the 3+1-dimensional case, the value of α can change the physics, and α must be chosen with care.

3.3.2 The Ergodic Moves

Our method of generating contributions to the path integral relies on generating a random, unlikely space-time and modifying it until it becomes a more likely space-time [3]. Therefore, it is important to have some way to change an arbitrary configuration of simplices into another configuration. To this end, we use the ergodic moves [3]. The moves are called ergodic because by composing them, one can go from any allowed space-time to any other allowed space-time.

Figure 6 shows the 5 ergodic moves for 2+1-dimensional CDT. The $(2,6)$ move acts on a $(3,1)$-simplex and a $(1,3)$-simplex; the $(3,1)$-simplex is split into three $(3,1)$-simplices and the

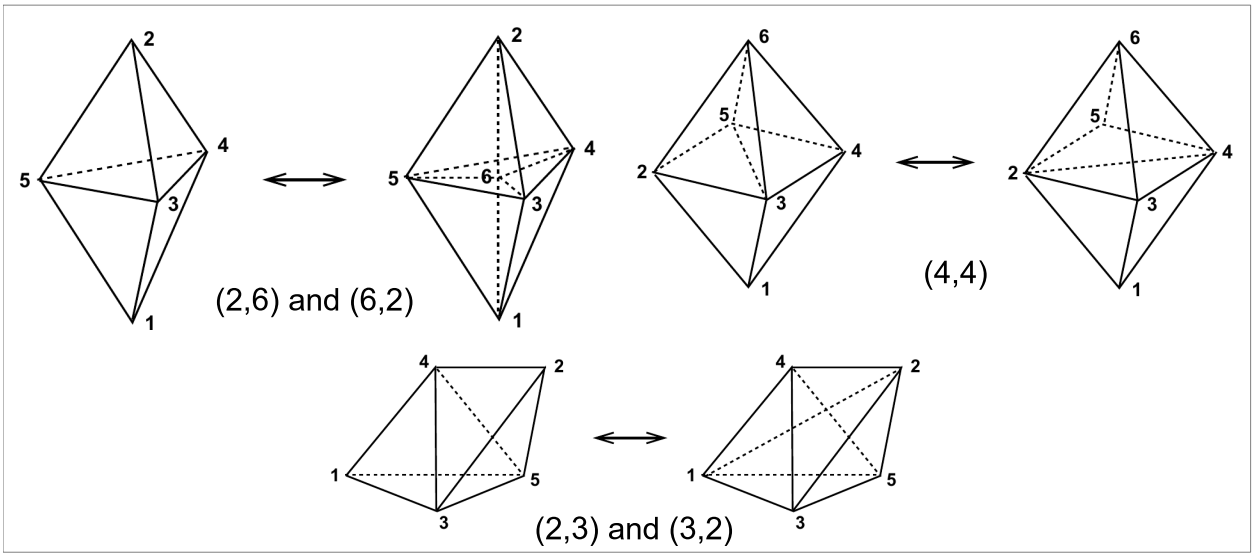

Figure 6: The ergodic moves in 2+1-dimensional CDT. Top left: The $(2,6)$ move and its inverse. Top right: The $(4,4)$ move, its own inverse. Bottom: The $(2,3)$ move and its inverse. Image from [3]

$(1,3)$-simplex is split into three $(1,3)$-simplices. The $(6,2)$ move is the inverse of the $(2,6)$ move. The $(4,4)$ move acts on two $(3,1)$-simplices and two $(1,3)$-simplices and is its own inverse; it simply rotates the edge shared by all four simplices by ninety degrees. The $(2,3)$ move acts on a $(2,2)$-simplex and either a $(3,1)$-simplex or a $(1,3)$-simplex; it adds an additional $(2,2)$-simplex to the complex. The $(3,2)$ move is the inverse of the $(2,3)$ move. For a more detailed description of the moves, see [3].

3.4 Performing the Path Integral

To quantize our discretized theory of gravity, we must build an ensemble of probable space-times and average over them. This amounts to performing the path integral discussed in section 2 [3]. The averaging process depends on what observable we wish to "measure." A specific example of this will be discussed later. The primary hurdle, however, is building an ensemble of space-times. For this, we rely on the Monte Carlo method and the Metropolis-Hastings algorithm [3].

The Metropolis algorithm as applied to CDT is as follows [3]:

1. Generate an arbitrary space-time constructed of equilateral simplices.
2. Randomly apply one of the ergodic moves to the space-time.
3. Calculate whether the new space-time is more or less likely than the old space-time, as given by its un-normalized weight in the path integral,[11] e^{iS}.

[11] Technically, the normalized weight $\frac{1}{Z}e^{iS}$ is the important quantity. However, since we only care about the ratio of

4. If the new space-time is more likely than the previous space-time, accept the change with probability $P = 1$. If it is less likely, accept the change with probability $P = P(new)/P(old)$.

5. Return to step 2.

To ensure that the probability amplitude is real and positive, we perform a Wick rotation on our space-time. A Wick rotation is a rotation of coordinates through the complex plane to change a Lorentzian manifold into a Euclidean one, with positive definite metric. We change the norm-squared of the time direction from negative to positive and pick up a factor of i [3].

After enough iterations of the Metropolis-Hastings algorithm, the frequency of each geometry will approach the frequencies given by the actual probability distribution. We perform this procedure and wait a sufficient amount of time a large number of times to produce a large ensemble of possible, relatively probable space-time geoemtries. We can average over these geometries to perform a path integral and calculate various observable quantities [3].

4 The Discrete Regge Action

To calculate probabilities, we need to calculate the discretized action, known as the Regge action. Ambørn and Loll first derived the action for 1+1, 2+1, and 3+1 dimensions [3]. The action for 2+1 dimensions with periodic boundary conditions in time is presented here. Later, when I discuss my own work, I will discuss the derivation for the action in 2+1 dimensions with the addition of the boundary term.

$$\begin{aligned} S^{(R)}_{EH}[\mathscr{T}_c] &= k\left[\frac{2\pi}{i}N_1^{SL} - \frac{3}{i}k\theta_{SL}^{(3,1)}\left(N_3^{(3,1)} + N_3^{(1,3)}\right) - \frac{2}{i}\theta_{SL}^{(2,2)}N_3^{(2,2)}\right] \\ &+ k\sqrt{\alpha}\left[2\pi N_1^{TL} - 3\theta_{TL}^{(3,1)}(N_3^{(3,1)} + N_3^{(1,3)}) - 4\theta_{TL}^{(2,2)}N_3^{(2,2)}\right] \\ &- \frac{\lambda}{12}\left[(N_3^{(3,1)} + N_3^{(1,3)})\sqrt{3\alpha+1} + N_3^{(2,2)}\sqrt{4\alpha+2}\right] \end{aligned} \tag{11}$$

Here, $k = \frac{1}{8\pi G}$ and $\lambda = \Lambda k$ are coupling constants. $-\alpha$ is the length-squared of a time-like vector. The N_x^y represents the number of simplices of a specific type. The subscript indicates the dimension of the simplices and the superscript indicates the type of simplex: SL for spacelike, TL for timelike, or (m,n) for a (m,n)-simplex of dimension 3. For example, the number of spacelike triangles is N_2^{SL} and the number of $(3,1)$-simplices is $N_3^{(3,1)}$. θ_x^y represents the dihedral angle of a simplex of a given type. The subscripts mean the same thing for angles as for numbers of simplices. Of course, the dihedral angles for a $(3,1)$-simplex are the same as the dihedral angles for a $(1,3)$-simplex, since they are the same angles, just on different time-slices. The first line comes from the summation over spacelike hinges, the second line comes from the summation over timelike hinges, and the third line comes from the summation over 3-simplices. Note that we could rewrite the second term of the first line using the relation $4N_1^{SL} = 3\left(N_3^{(1,3)} + N_3^{(3,1)}\right)$ [3].

weights, the factor of $1/Z$ cancels out. This is fortunate, since we don't know what Z is—if we did, we could simply perform the path integral.

Although it is not used here, we will introduce the following notation.

$$V_3^{(2,2)} = \frac{1}{12}\sqrt{2\alpha+1} \text{ and} \tag{12}$$

$$V_3^{(3,1)} = V_3^{(1,3)} = \frac{1}{12}\sqrt{3\alpha+1}, \tag{13}$$

where $V_3^{(2,2)}$ is the 3-dimensional volume of a $(2,2)$-simplex and $V_3^{(3,1)}$ is the 3-dimensional volume of a $(3,1)$ or $(1,3)$ simplex. At first it seems like $(3,1)$ and $(2,2)$ simplices should have the same 3-volume, since they're the same up to rigid motion. However, rigid motion matters in this case because the metric is Lorentzian. Timelike links have negative length, and it matters whether the simplex has greater spacelike extent or timelike extent.

By plugging this action into the partition function, the theory of 2+1-dimensional CDT for fixed boundary conditions is complete. Next, we will discuss my research and my results.

5 My Research

This section discusses my contributions to CDT in 2+1 dimensions. I derived the discrete Regge action for a space-time where the boundaries are not identified. Instead, the initial and final time slices are held fixed with spatial geometries defined by the physicist. I also implemented changes to our group's CDT simulation code that held these boundaries fixed. A previous student, David Kemansky, also worked on this problem, and I would not have finished my project without the contributions from David's work.

First, I will describe the derivation of the Regge action in some depth. This derivation differs from that of Ambjørn and Loll [3] because we include the boundary term. Then I will describe the results of my project. I will not describe the details of the programming work here, but I am working on a programmer's guide for future students to use to modify my code.

5.1 An Aside on Extrinsic Curvature

Before we can discuss the actual derivation of the action, we need to discuss the discretization of extrinsic curvature. Extrinsic curvature is the trace of the Second Fundamental Form—mathematicians might recognize it as mean curvature. Extrinsic curvature is so called because it depends on the embedding of the manifold in a larger space, while intrinsic curvature (i.e., Riemann curvature) depends only on the metric. Hartle and Sorkin propose that

$$\int_{\partial\mathscr{M}} d^{D-1}\sqrt{\gamma}K = \sum_{b\in\partial\mathscr{M}} V(b)\psi(b), \tag{14}$$

where γ is the *induced metric*[12], K is the extrinsic curvature, $V(b)$ is the $(D-2)$-dimensional analogue of volume of a bone in the boundary, and $\psi(b)$ is the deficit angle of the bone[17]. Deficit angle works somewhat differently on the boundary than it does in the bulk.

[12]The induced metric is the metric inherited by the ambient metric and the embedding of the manifold.

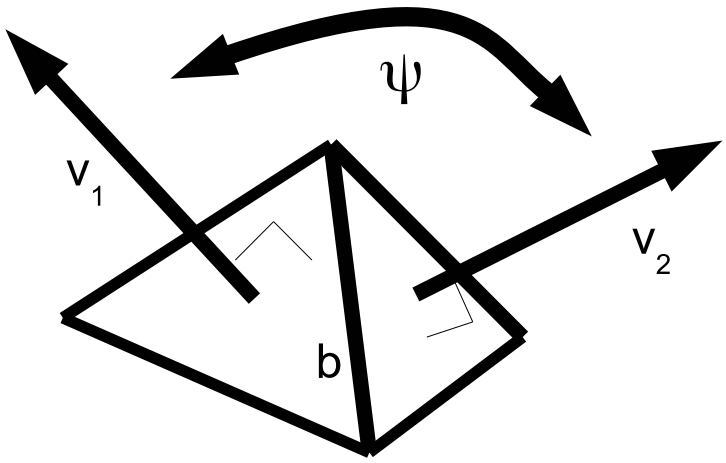

Figure 7: Finding the deficit angle on the boundary. The angle between the two vectors v_1 and v_2 is proportional to $\pi - \psi(b)$, where $\psi(b)$ is the deficit angle around the bone b.

In the boundary, we parallel transport a vector v_1 normal to the boundary across a bone from one $(D-1)$-dimensional simplex in our triangulation of the boundary to an adjacent one, where it becomes v_2, as shown in figure 7 [17]. If $K = 0$ and the space is flat, v_1 is parallel to v_2 and the deficit angle is zero. If $K \neq 0$, then the deficit angle ψ is the angle between v_1 and v_2 [17].

5.2 Overview of the Discrete Action

For a $(2+1)$-dimensional space-time manifold[13] $\mathscr{M}$ with boundary $\partial\mathscr{M}$, we must add to the Einstein-Hilbert action [12],

$$S_{EH}[\mathbf{g}] = \frac{1}{16\pi G}\int_{\mathscr{M}} \mathrm{d}^3x\sqrt{-g}\,(R-2\Lambda)\,, \tag{15}$$

the Gibbons-Hawking-York boundary term [13],

$$S_{GH}[\gamma] = \frac{1}{8\pi G}\int_{\partial\mathscr{M}} \mathrm{d}^2y\sqrt{|\gamma|}K. \tag{16}$$

Here, γ is the induced metric on the boundary $\partial\mathscr{M}$ and K is the trace of the extrinsic curvature of the boundary $\partial\mathscr{M}$. Regge demonstrated that, for a triangulated space-time manifold $\mathscr{T}$, the Einstein-Hilbert action assumes the form [15]

$$S^{(R)}_{EH}[\mathscr{T}] = \frac{1}{8\pi G}\sum_{h\in\mathscr{T}} A_h\delta_h - \frac{\Lambda}{8\pi G}\sum_{s\in\mathscr{T}} V_s. \tag{17}$$

Here, h is a 1-dimensional hinge having area A_h and deficit angle δ_h, while V_s is the space-time volume of a 3-simplex s. Hartle and Sorkin demonstrated that, for a triangulated space-time manifold

[13] From now on, we will be working in 2+1 dimensions. D is no longer arbitrary.

$\mathscr{T}$ with boundary $\partial\mathscr{T}$, the Gibbons-Hawking-York boundary term assumes the form [17]

$$S^{(R)}_{GH}[\partial\mathscr{T}] = \frac{1}{8\pi G}\sum_{h\in\partial\mathscr{T}} A_h\psi_h. \tag{18}$$

Here, h is a 1-dimensional hinge on the boundary $\partial\mathscr{T}$ having area A_h and ψ_h is the angle between the two vectors normal to the two spacelike 2-simplices intersecting at the hinge h.

We wish to determine the form of the Regge-Einstein-Hilbert action supplemented by the Regge-Gibbons-Hawking-York boundary term in $(2+1)$-dimensional causal dynamical triangulations for two-sphere spatial topology and line interval temporal topology.

5.3 The Bulk Action

If the Regge-Einstein-Hilbert action for $(2+1)$-dimensional causal dynamical triangulations (CDT) is to include a boundary term, it must be split into a bulk term and a boundary term. Hartle and Sorkin provide the framework for the Gibbons-Hawking-York boundary term [17]. However, we must first ensure that the Regge-Einstein-Hilbert action does not take any boundary terms as input. We will re-derive the Regge-Einstein-Hilbert action, making sure we don't count any part of the boundary. This is the *bulk action*.

We start with the CDT version of the Regge action [15] given by Ambjørn *et al.* [3]:

$$\begin{aligned} S^{R}_{EH}[\mathscr{T}_{bulk}] \;=\; & k\sum_{\substack{\text{space-like}\\ \text{links } l}} Vol(l)\frac{1}{i}\left(2\pi - \sum_{\substack{\text{tetrahedra}\\ \text{at } l\\ t}}\theta_D(t,l)\right) \\ & +k\sum_{\substack{\text{time-like}\\ \text{links } l}} Vol(l)\left(2\pi - \sum_{\substack{\text{tetrahedra}\\ \text{at } l\\ t}}\theta_D(t,l)\right) \\ & -\lambda\sum_{\substack{(3,1) \text{ and } (1,3)\\ \text{tetrahedra}}} V_3^{(3,1)} - \lambda\sum_{\substack{(2,2)\\ \text{tetrahedra}}} V_3^{(2,2)}. \end{aligned} \tag{19}$$

Here $Vol(l)$ is the volume of a given link l. Because we are in $(2+1)$-dimensions, we can assume that $Vol(l) = 1$ for space-like links and that $Vol(l) = \sqrt{\alpha}$ for time-like links. $\theta_D(t,l)$ is the dihedral angle of a tetrahedron t around a link l. $V_3^{(2,2)}$ and $V_3^{(3,1)}$ are the volumes of $(2,2)-$ and $(3,1)-$ tetrahedra respectively. These values are given in Ambjørn *et al* [3].

If we distribute summation signs and perform obvious summations, we find that:

$$\begin{aligned} S^R_{EH}[\mathscr{T}_{bulk}] &= \frac{2\pi k}{i}\left[N_1^{SL}(\mathscr{T}) - N_1^{SL}(S_i^{(2)}) - N_1^{SL}(S_f'^{(2)})\right] - \frac{k}{i}\sum_{\substack{\text{space-like}\\ \text{links } l}}\sum_{\substack{\text{tetrahedra } t\\ \text{at link } l}}\theta_D(t,l) \\ &\quad +2\pi k\sqrt{\alpha}N_1^{TL} - k\sqrt{\alpha}\sum_{\substack{\text{time-like}\\ \text{links } l}}\sum_{\substack{\text{tetrahedra } t\\ \text{at link } l}}\theta_D(t,l) \\ &\quad -\lambda\left[V_3^{(3,1)}(N_3^{(3,1)}+N_3^{(1,3)}) + V_3^{(2,2)}N_3^{(2,2)}\right], \end{aligned} \tag{20}$$

where $N_1^{SL}(S_i^{(2)})$ is the number of space-like links that lie in the initial surface at proper time $\tau = 0$. $S^{(2)}$ simply indicates that the topology of the surface is spherical. Likewise, $N_1^{SL}(S_f'^{(2)}$ is the number of space-like links that lie in the final surface at proper time $\tau = \tau_{final}$. We perform the subtraction in the first term to avoid over-counting objects in the boundary. $V_3^{(3,1)}$ and $V_3^{(2,2)}$ are the 3-volumes of $(3,1)$ (and likewise $(1,3)$) tetrahedra and $(2,2)$ tetrahedra respectively.

We now need to count the number of tetrahedra connected to each link and sum over all links. To perform this operation, we first act out the inner sum over dihedral angles around an individual link:

$$\begin{aligned} S^R_{EH}[\mathscr{T}_{bulk}] &= \frac{2\pi k}{i}\left[N_1^{SL}(\mathscr{T}) - N_1^{SL}(\mathscr{S}_i^{(2)}) - N_1^{SL}(\mathscr{S}_f'^{(2)})\right] \\ &\quad -\frac{k}{i}\sum_{\substack{\text{space-like}\\ \text{links } l\\ \text{in bulk}}}\left[N_3^{(2,2)}(l)\theta_{SL}^{(2,2)} + N_3^{(1,3)}(l)\theta_{SL}^{(3,1)} + N_3^{(3,1)}(l)\theta_{SL}^{(1,3)}\right] \\ &\quad +2\pi k\sqrt{\alpha}N_1^{TL} - k\sqrt{\alpha}\sum_{\substack{\text{time-like}\\ \text{links } l}}\left[N_3^{(2,2)}(l)\theta_{TL}^{(2,2)} + N_3^{(1,3)}(l)\theta_{TL}^{(3,1)} + N_3^{(3,1)}(l)\theta_{TL}^{(3,1)}\right] \\ &\quad -\lambda\left[V_3^{(3,1)}(N_3^{(3,1)}+N_3^{(1,3)}) + V_3^{(2,2)}N_3^{(2,2)}\right], \end{aligned} \tag{21}$$

where $N_3^{(2,2)}(l)$, $N_3^{(3,1)}(l)$, and $N_3^{(1,3)}(l)$ are the number of $(2,2)-$, $(3,1)-$, and $(1,3)-$tetrahedra respectively around a given link. To perform the remaining summation over the entire manifold, we look at how many links that each tetrahedron connects to and sum over tetrahedra, rather than summing over tetrahedra at each link and then summing over tetrahedra. We know that:

- Each $(2,2)-$simplex connects to two space-like links in the bulk, but only one on each boundary. Thus:

$$\sum_{\substack{\text{space-like}\\ \text{links } l\\ \text{in bulk}}} N_3^{(2,2)}(l) = 2N_3^{(2,2)}(\mathscr{T}_{bulk})$$

  and

$$\sum_{\substack{\text{space-like}\\ \text{links } l\\ \text{in boundary}}} N_3^{(2,2)}(l) = N_3^{(2,2)}(\mathscr{S}_i^{(2)}) + N_3^{(2,2)}(\mathscr{S}_f'^{(2)}),$$

where $N_3^{(2,2)}(\mathscr{T}_{bulk})$ is the total number of $(2,2)-$simplices in the manifold that do not connect to a link in the boundary. Likewise, $N_3^{(2,2)}(\mathscr{S}_i^{(2)})$ and $N_3^{(2,2)}(\mathscr{S}_f'^{(2)})$ are the total number of simplices that have at least one link (in fact exactly one) in the initial boundary or the final boundary respectively. We will continue to use this naming convention. Thus:

$$\sum_{\substack{\text{space-like}\\ \text{links } l\\ \text{in bulk}}} N_3^{(2,2)}(l) = 2N_3^{(2,2)}(\mathscr{T}_{bulk}) = N_3^{(2,2)} - N_3^{(2,2)}(\mathscr{S}_i^{(2)}) - N_3^{(2,2)}(\mathscr{S}_f'^{(2)}), \tag{22}$$

where $N_3^{(2,2)}$ is the total number of $(2,2)$-simplices in the manifold.

- Each $(2,2)-$simplex connects to four time-like links. Thus:

$$\sum_{\substack{\text{time-like}\\ \text{links } l}} N_3^{(2,2)}(l) = 4N_3^{(2,2)}. \tag{23}$$

There are no time-like links in the boundary, so will ignore this distinction.

- Each $(3,1)-$ and each $(1,3)-$simplex in bulk connects to three spacelike links. Thus

$$\sum_{\substack{\text{space-like}\\ \text{links } l\\ \text{in bulk}}} \left(N_3^{(3,1)} + N_3^{(1,3)}\right) = 3\left(N_3^{(3,1)}(\mathscr{T}_{bulk}) + N_3^{(1,3)}(\mathscr{T}_{bulk})\right).$$

On the initial boundary, each $(3,1)-$simplex connects to three links, but no $(1,3)-$simplex connects to any links at all. Similarly, on the final boundary, each $(1,3)-$simplex connects to 3 links but no $(3,1)-$simplex connects to any. Thus:

$$\sum_{\substack{\text{space-like}\\ \text{links } l\\ \text{on-boundary}}} (N_3^{(3,1)}(l) + N_3^{(1,3)}(l)) = 3\left(N_3^{(3,1)}(\mathscr{S}_i^{(2)}) + N_3^{(1,3)}(\mathscr{S}_f'^{(2)}\right).$$

Thus:

$$\begin{aligned}\sum_{\substack{\text{space-like}\\ \text{links } l\\ \text{in bulk}}} \left(N_3^{(3,1)} + N_3^{(1,3)}\right) &= 3\left(N_3^{(3,1)}(\mathscr{T}_{bulk}) + N_3^{(1,3)}(\mathscr{T}_{bulk})\right)\\ &= 3\left(N_3^{(3,1)} + N_3^{(1,3)}\right)\\ &\quad -3\left(N_3^{(3,1)}(\mathscr{S}_i^{(2)}) + N_3^{(1,3)}(\mathscr{S}_f'^{(2)})\right).\end{aligned} \tag{24}$$

- Each $(3,1)-$ or $(1,3)-$simplex connects to 3 time-like links. Thus:

$$\sum_{\substack{\text{time-like}\\ \text{links } l}} \left(N_3^{(3,1)}(l) + N_3^{(1,3)}(l)\right) = 3\left(N_3^{(3,1)} + N_3^{(1,3)}\right). \tag{25}$$

There are no time-like links in the boundary.

If we take the counting relations given above into account, then we find that

$$
\begin{aligned}
S^R_{EH}[\mathscr{T}_{bulk}] \;=\; & \frac{2\pi k}{i}\left[N_1^{SL}(\mathscr{T}) - N_1^{SL}(\mathscr{S}_i^{(2)}) - N_1^{SL}(\mathscr{S}_f^{\prime(2)})\right] \\
& -\frac{k}{i}\theta_{SL}^{(2,2)}\left[\left(2N_3^{(2,2)} - N_3^{(2,2)}(\mathscr{S}_i^{(2)}) - N_3^{(2,2)}(\mathscr{S}_f^{\prime(2)})\right)\right] \\
& -\frac{3k}{i}\theta_{SL}^{(1,3)}\left[N_3^{(1,3)} + N_3^{(3,1)}) - N_3^{(3,1)}(\mathscr{S}_i^{(2)}) - N_3^{(1,3)}(\mathscr{S}_f^{\prime(2)})\right] \\
& +2\pi k\sqrt{\alpha}N_1^{TL} - k\sqrt{\alpha}\left[4\theta_{TL}^{(2,2)}N_3^{(2,2)} + 3\theta_{TL}^{(3,1)}\left(N_3^{(3,1)} + N_3^{(1,3)}\right)\right] \\
& -\lambda\left[V_3^{(3,1)}(N_3^{(3,1)} + N_3^{(1,3)}) + V_3^{(2,2)}N_3^{(2,2)}\right].
\end{aligned}
\tag{26}
$$

This is the bulk form of the Regge action.

5.4 The Gibbons-Hawking-York Term

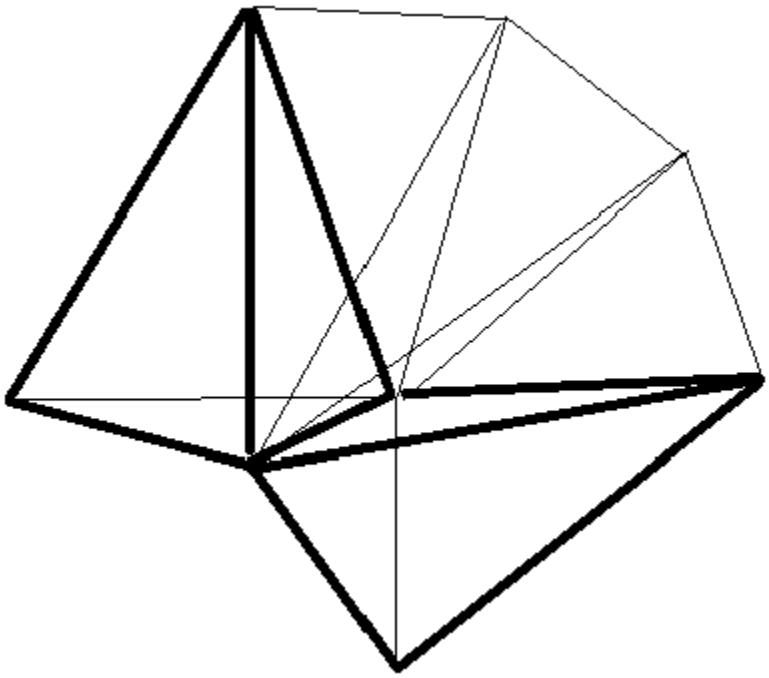

Figure 8: $(2,2)$-simplices are the source of extrinsic curvature on the boundary. In parallel transporting the vector normal to one component to the boundary between two spacelike 2-simplices intersecting at the bone b (or hinge h), the vector rotates through twice the dihedral angle of a $(3,1)$-simplex and through the dihedral angle of a $(2,2)$-simplex a number of times equal to however many 2-simplices are connected to the bone b.

We now supplement the Regge-Einstein-Hilbert action for $(2+1)$-dimensional causal dynamical triangulations with the appropriate Regge-Gibbons-Hawking-York boundary term. Given the desired space-time topology, the boundary $\partial\mathscr{T}_c$ consists of two disconnected components: an initial (or past) spatial two-sphere $\mathscr{S}_i^2$ and a final (or future) spatial two-sphere $\mathscr{S}_f^2$. Based on the demonstration of Hartle and Sorkin [17], we propose the prescription

$$\begin{aligned} S_{GH}^{(R)}[\partial\mathscr{T}_c] &= \frac{1}{8\pi G}\sum_{h\in\mathscr{S}_i^2}\frac{1}{i}\left[\pi - 2\theta_{SL}^{(3,1)} - \theta_{SL}^{(2,2)}N_{3\uparrow}^{(2,2)}(h)\right] \\ &\quad + \frac{1}{8\pi G}\sum_{h\in\mathscr{S}_f^2}\frac{1}{i}\left[\pi - 2\theta_{SL}^{(1,3)} - \theta_{SL}^{(2,2)}N_{3\downarrow}^{(2,2)}(h)\right]. \end{aligned} \tag{27}$$

Here, $N_{3\uparrow}^{(2,2)}(h)$ is the number of future-directed $(2,2)$ 3-simplices attached to the hinge h and $N_{3\downarrow}^{(2,2)}(h)$ is the number of past-directed $(2,2)$ 3-simplices attached to the hinge h. We justify this prescription as follows. In parallel transporting the vector normal to one component of the boundary $\partial\mathscr{T}_c$ between two spacelike 2-simplices intersecting at the hinge h, the vector rotates through the angle

$$\frac{1}{i}\left[2\theta_{SL}^{(3,1)} + \theta_{SL}^{(2,2)}N_3^{(2,2)}(h)\right], \tag{28}$$

as shown in figure 8. When this angle is $\frac{\pi}{i}$, the extrinsic curvature vanishes locally at the hinge h; this fact dictates the deficit angle-like form of our above prescription. The absence of a relative negative sign between the contributions of the two disconnected components of the boundary $\partial\mathscr{T}_c$ to the Regge-Gibbons-Hawking-York boundary term stems from the fact that the future-directed orientation of the vector normal to $\mathscr{S}_i^2$ and the past-directed orientation of the vector normal to $\mathscr{S}_f^2$ are accounted for in the past-directed and future-directed orientations of the $(2,2)$ 3-simplices attached to the boundary. Performing the summations over the hinges on the boundary $\partial\mathscr{T}_c$, we may rewrite the Regge-Gibbons-Hawking-York boundary term as

$$\begin{aligned} S_{GH}^{(R)}[\partial\mathscr{T}_c] &= \frac{1}{8\pi G}\left[\frac{\pi}{i}N_1^{SL}(\mathscr{S}_i^2) - \frac{2}{i}\theta_{SL}^{(3,1)}N_1^{SL}(\mathscr{S}_i^2) - \frac{1}{i}\theta_{SL}^{(2,2)}N_{3\uparrow}^{(2,2)}(\mathscr{S}_i^2)\right] \\ &\quad + \frac{1}{8\pi G}\left[\frac{\pi}{i}N_1^{SL}(\mathscr{S}_f^2) - \frac{2}{i}\theta_{SL}^{(3,1)}N_1^{SL}(\mathscr{S}_f^2) - \frac{1}{i}\theta_{SL}^{(2,2)}N_{3\downarrow}^{(2,2)}(\mathscr{S}_f^2)\right]. \end{aligned} \tag{29}$$

The complete Regge action is thus

$$
\begin{aligned}
S^{(R)}[\mathscr{T}_c] \;=\; & \frac{2\pi k}{i}\left[N_1^{SL}(\mathscr{T}) - N_1^{SL}(\mathscr{S}_i^{(2)}) - N_1^{SL}(\mathscr{S}_f'^{(2)})\right] \\
& \quad -\frac{k}{i}\theta_{SL}^{(2,2)}\left[\left(2N_3^{(2,2)} - N_3^{(2,2)}(\mathscr{S}_i^{(2)}) - N_3^{(2,2)}(\mathscr{S}_f'^{(2)})\right)\right] \\
& \quad -\frac{3k}{i}\theta_{SL}^{(1,3)}\left[N_3^{(1,3)} + N_3^{(3,1)}) - N_3^{(3,1)}(\mathscr{S}_i^{(2)}) - N_3^{(1,3)}(\mathscr{S}_f'^{(2)})\right] \\
& + 2\pi k\sqrt{\alpha}N_1^{TL} - k\sqrt{\alpha}\left[4\theta_{TL}^{(2,2)}N_3^{(2,2)} + 3\theta_{TL}^{(3,1)}\left(N_3^{(3,1)} + N_3^{(1,3)}\right)\right] \\
& - \lambda\left[V_3^{(3,1)}(N_3^{(3,1)} + N_3^{(1,3)}) + V_3^{(2,2)}N_3^{(2,2)}\right]. \qquad (30) \\
& + \frac{1}{8\pi G}\left[\frac{\pi}{i}N_1^{SL}(\mathscr{S}_i^2) - \frac{2}{i}\theta_{SL}^{(3,1)}N_1^{SL}(\mathscr{S}_i^2) - \frac{1}{i}\theta_{SL}^{(2,2)}N_{3\uparrow}^{(2,2)}(\mathscr{S}_i^2)\right] \\
& + \frac{1}{8\pi G}\left[\frac{\pi}{i}N_1^{SL}(\mathscr{S}_f^2) - \frac{2}{i}\theta_{SL}^{(3,1)}N_1^{SL}(\mathscr{S}_f^2) - \frac{1}{i}\theta_{SL}^{(2,2)}N_{3\downarrow}^{(2,2)}(\mathscr{S}_f^2)\right].
\end{aligned}
$$

5.5 Consistency Checks

Next, we demonstrate that our prescription for the Regge-Gibbons-Hawking-York boundary term in $(2+1)$-dimensional causal dynamical triangulations is consistent with the form of the Regge-Einstein-Hilbert action determined by Ambjørn *et al*. We make such a demonstration by verifying that our prescription for the Regge-Gibbons-Hawking-York boundary term reproduces the Regge-Einstein-Hilbert action when we compose two space-time regions sharing a common boundary $\mathscr{S}_c^2$. Consider two triangulated space-time manifolds $\mathscr{T}_c$ and $\mathscr{T}_c'$ both with two-sphere spatial topology and line interval temporal topology. The boundary $\partial\mathscr{T}_c$ consists of an initial two-sphere $\mathscr{S}_i^2$ and a final two-sphere $\mathscr{S}_f^2$, and the boundary $\partial\mathscr{T}_c'$ consists of an initial two-sphere $\mathscr{S}_i'^2$ and a final two-sphere $\mathscr{S}_f'^2$. To compose the two triangulated space-time manifolds $\mathscr{T}_c$ and $\mathscr{T}_c'$, we first take the two-spheres $\mathscr{S}_f^2$ and $\mathscr{S}_i'^2$ to have the same intrinsic geometry, then orient the two-spheres $\mathscr{S}_f^2$ and $\mathscr{S}_i'^2$ to have coincident normal vectors. We may thus identify these two two-spheres as $\mathscr{S}_c^2$. The Regge-Gibbons-Hawking-York boundary term contributions of $\mathscr{S}_c^2$ from the two triangulated space-time manifolds $\mathscr{T}_c$ and $\mathscr{T}_c'$ are

$$
\begin{aligned}
& \frac{1}{8\pi G}\left[\frac{\pi}{i}N_1^{SL}(\mathscr{S}_f^2) - \frac{2}{i}\theta_{SL}^{(3,1)}N_1^{SL}(\mathscr{S}_f^2) - \frac{1}{i}\theta_{SL}^{(2,2)}N_{3\downarrow}^{(2,2)}(\mathscr{S}_f^2)\right] \\
& + \frac{1}{8\pi G}\left[\frac{\pi}{i}N_1^{SL}(\mathscr{S}_i'^2) - \frac{2}{i}\theta_{SL}^{(3,1)}N_1^{SL}(\mathscr{S}_i'^2) - \frac{1}{i}\theta_{SL}^{(2,2)}N_{3\uparrow}^{(2,2)}(\mathscr{S}_i'^2)\right]. \qquad (31)
\end{aligned}
$$

Together these two Regge-Gibbons-Hawking-York boundary terms combine to give the contribution to the Regge-Einstein-Hilbert action coming from the spacelike hinges on $\mathscr{S}_c^2$.

5.6 Preliminary Results For Fixed Boundaries

So far, we have described the basic methods for CDT in 2+1 dimensions and derived the action required for fixed-boundaries. We will now present results for fixed boundaries CDT simulations and compare them to periodic-boundary simulations of the past. As discussed in section 3.4, the averaging process for the path integral depends on what observable we wish to examine. Observables must relate to ensembles rather than to individual space-times. Quantum mechanics is inherently probabilistic and this is as close as an experimenter can get. In this work, we discuss spatial extent as a function of proper time. In other words, we count the number of space-like triangles at each time slice for each space-time in an ensemble and average over this value to find an expected "shape" for the universe. The standard deviation of this value can be thought of as the quantum fluctuations around the mean, or as the variance of the observable.

Simulations are performed for a fixed size of the universe—i.e., a fixed number of time slices and a fixed number of tetrahedra. We vary the values of G and Λ, whether the boundaries are fixed to some geometry, or whether they are periodic. The topology of the spatial universe at each proper time is homeomorphic to a two-sphere S^2.

It is important to adjust G and Λ so that the probability of a volume increasing move being accepted is equal to the probability of a volume-decreasing move being accepted. This is because the stability of the number of 3-simplices in the space-time depends on the simulation not preferring one type of change in volume over any others. If we do not reach a steady state, the number of 3-simplices in a space-time will approach either infinity or zero and the simulation will be useless.

5.6.1 The Periodic Boundary Conditions Case

In the past, all CDT simulations were performed with periodic boundary conditions in time. In other words, the geometries at the initial and final times were identified. This method produced two "phases" of geometry based on the values of G and Λ. So-called "Phase A" concentrates all spatial extent into one or two time slices, surrounded by thin "stalks"in which each time slice contains only 4 space-like triangles—the minimal possible number required to be homeomorphic to the sphere.

"Phase C" is more interesting. The spatial extent of the universe in phase C has the same functional form as the Wick-rotated shape of de Sitter space. Figure 9 shows an example of Phase C in the periodic boundary conditions case. Because all time slices are identical in the periodic time case, the bulk of the space-time (the $\cos^2(t)$ shape) can be centered on any time slice. To compare space-times in an ensemble, a coordinate transform must be performed on each space-time in an ensemble such that the bulk forms in the center of the coordinate system and the space-times can be averaged. Although the functional form of the bulk conforms to the classical solution to Einstein's equations for an empty universe, the long "stalks" present in Phase A are present. These stalks are non-classical and impossible to remove in the periodic boundary conditions case.

5.6.2 The Fixed Boundary Conditions Case

So far, for the fixed boundaries case, we have found Phase A and Phase C for approximately the same coupling-constant values as for the periodic boundary conditions case. We have yet to find

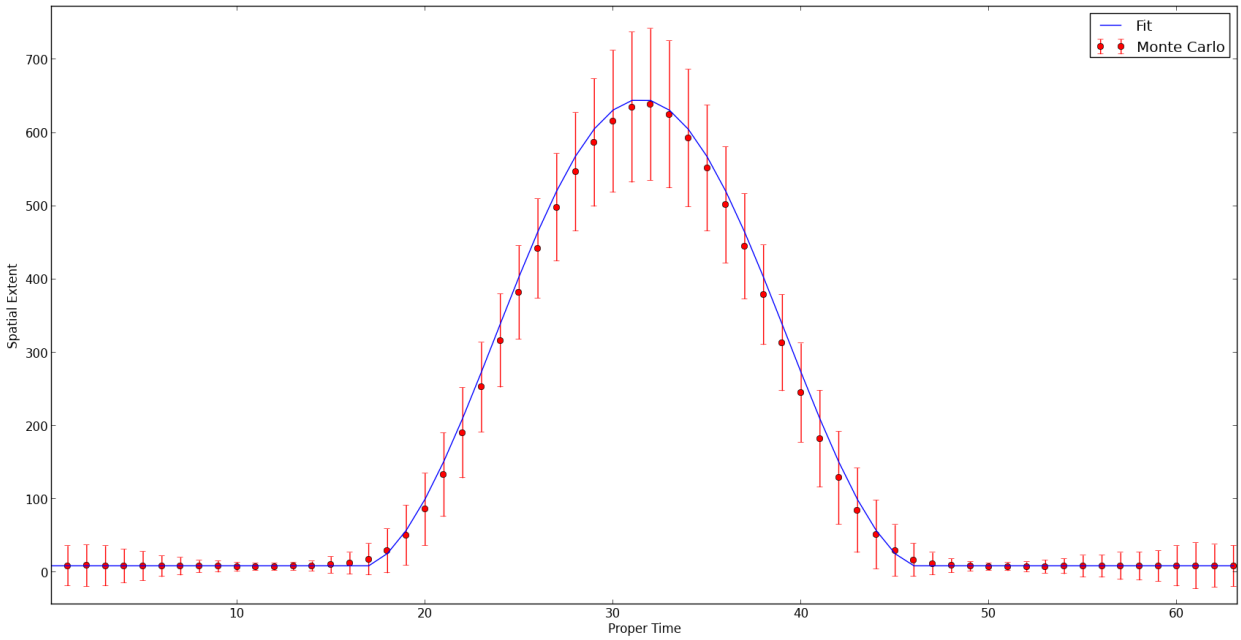

Figure 9: An example of Phase C in the periodic boundary conditions case. The x-axis is proper time and the y-axis is the number of space-like triangles at a given time. The data points are the average over a large ensemble of space-times. The error bars are the standard deviation. The line is a fit to the functional form for Wick-rotated de Sitter space.

the critical values at which a phase transition occurs. If we set each boundary to be only four space-like triangles (i.e., a tetrahedron) and use the exact same number of 3-simplices, number of time slices, and values for G and Λ, we reproduce the results for periodic boundary conditions exactly, as shown in figure 10.

However, with fixed boundaries, we can eliminate the stalks. If we choose the geometry at proper time $t = 12$ in figure 10 to be the boundary at time $t = 0$, choose the geometry at $t = 41$ to be our boundary at the final time, and allow for only 29 time slices, we can generate a space-time ensemble whose average fits the classical solution very closely indeed, as shown in figure 11. To our knowledge, eliminating the stalks has not been done with periodic boundary conditions. This might indicate that fixed boundary conditions offer a more accurate picture of quantum gravity.

6 Outlook

So far, we have derived the discretized Regge action for the CDT in 2+1 dimensions in the fixed boundary condition case and demonstrated that fixed-boundaries CDT can reproduce—and, in fact, improve upon—results from periodic-boundary CDT. The level of control offered by fixed-boundaries CDT hints that there might be interesting physics waiting to be explored with fixed boundary conditions. One possibility is to explore the de Sitter length of simulated space-times

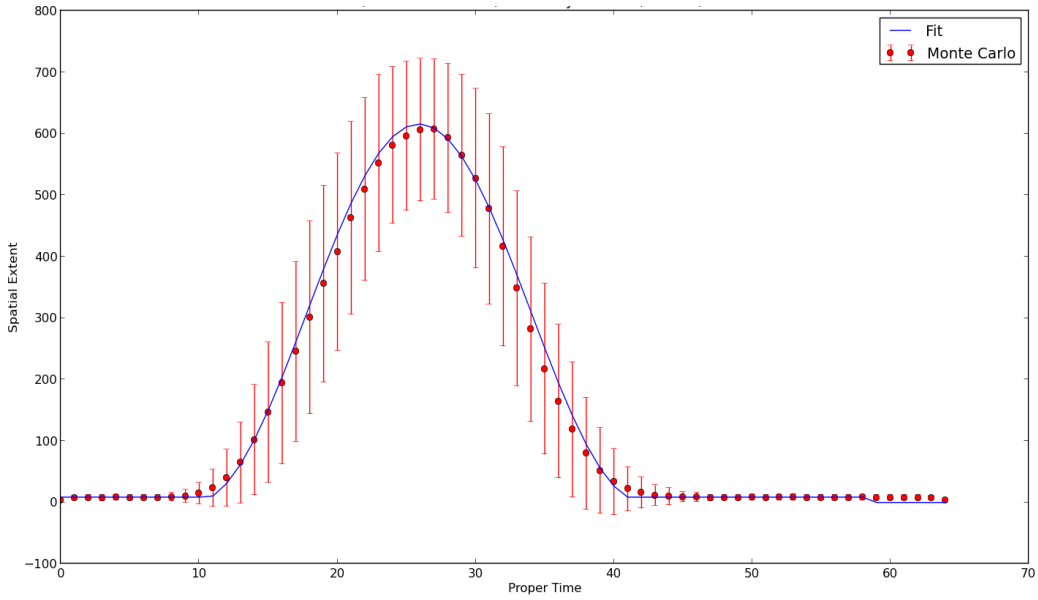

Figure 10: An example of Phase C with fixed boundary conditions. Each boundary has 4 space-like triangles in it.

in Phase C and find the most probable de Sitter length by varying the number of time slices in the simulation. Another possibility is to keep one boundary fixed and vary the other boundary over a wide number of geometries. By looking at the action, we could calculate the probability that a space-time starting from a minimal initial geometry evolves into some final geometry. This transition probability is known as the Hartle-Hawking wave function, and fixed boundaries CDT might allow us to explore it in great depth.

7 Acknowledgments

I would like to thank Joshua Cooperman, with whom I worked closely, for his help, guidance, friendship, and many valuable discussions. I'd like to thank Professor Steve Carlip, my advisor on this project, which would not have been possible without his patience, enthusiasm, and guidance. I'd also like to thank Rajesh Kommu, David Kamensky, and Christian Anderson, who worked on the CDT code before me and from whose prior efforts I greatly benefited. Finally, I'd like to thank the NSF and the REU program and its coordinators, especially Professor Rena Zieve, for making my summer of studying quantum gravity possible. It's been one of the best experiences of my life.

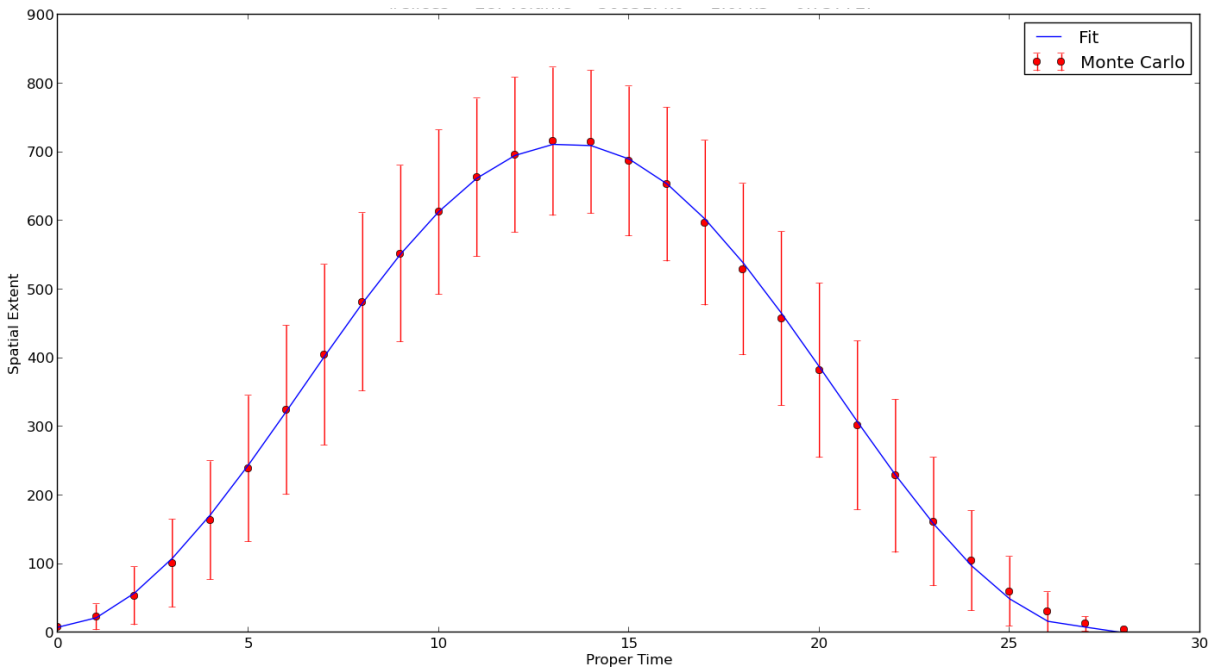

Figure 11: An example of Phase C with fixed boundary conditions. The boundaries and simulation parameters have been chosen so as to eliminate the non-classical stalks—a feat which is, to our knowledge, impossible with periodic boundary conditions.

References

[1] R. Loll. The emergence of spacetime or quantum gravity on your desktop. *Classical and Quantum Gravity*, 25(11), 2008.

[2] M. K. Sachs. Testing lattice quantum gravity in 2+1 dimensions. *arXiv*, 2011.

[3] J. Ambjørn, J. Jurkiewicz, and R. Loll. Dynamically triangulating lorentzian quantum gravity. *Nuclear Physics B*, 610:347–382, 2001.

[4] J. Ambjørn, J. Jurkiewicz, and R. Loll. Emergence of a 4d world from causal quantum gravity. *Physical Review Letters*, 93(131301), 2004.

[5] J. Ambjørn, J. Jurkiewicz, and R. Loll. The self-organized quantum de sitter universe. *arXiv*, 2008.

[6] R. Kommu. A validation of causal dynamical triangulations. *arXiv*, 2011.

[7] J. Ambjørn et al. Cdt—an entropic theory of quantum gravity. *arXiv*, 2010.

[8] J. Ambjørn, J. Jurkiewicz, and R. Loll. Causal dynamical triangulations and the quest for quantum gravity. *arXiv*, 2010.

[9] C. Anderson and Others. Quantizing horava-lifshitz gravity via causal dynamical triangulations. *Physical Review D*, 85(044027), 2012.

[10] J. Ambjørn, J. Jurkiewicz, and R. Loll. The spectral dimension of the universe is scale dependent. *Physical Review Letters*, 95(171301), 2005.

[11] R. Shankar. *Principles of Quantum Mechanics*. Springer, United States, 1994.

[12] C. W. Misner, K. S. Thorne, and J. A. Wheeler. *Gravitation*. W. H. Freeman and Company, San Francisco, 1973.

[13] E. Poisson. *A Relativist's Toolkit: The Mathematics of Black-Hole Mechanics*. Cambridge University Press, New York, 2004.

[14] S. M. Carroll. *Spacetime and Geometry*. Addison Wesley, San Francisco, 2004.

[15] T. Regge. General relativity without coordinates. *Nuovo Cimento*, 19(3):558–571, 1961.

[16] J. Oprea. *Differential Geometry and Its Applications*. The Mathematical Association of America, United States, 2007.

[17] J.B. Hartle and R. Sorkin. Boundary term in the action for the regge calculus. *General Relativity and Gravitation*, 13(6):541–549, 1981.